ACS APPLIED MATERIALS & INTERFACES

Research Article

www.acsami.org

Optofluidic Microreactors with TiO_2-Coated Fiberglass

Lin Li, Rong Chen,* Xun Zhu, Hong Wang, Yongzhong Wang, Qiang Liao, and Dongye Wang

Key Laboratory of Low-grade Energy Utilization Technologies and Systems (Chongqing University), Ministry of Education, Chongqing 400030, China

Institute of Engineering Thermophysics, Chongqing University, Chongqing 400030, China

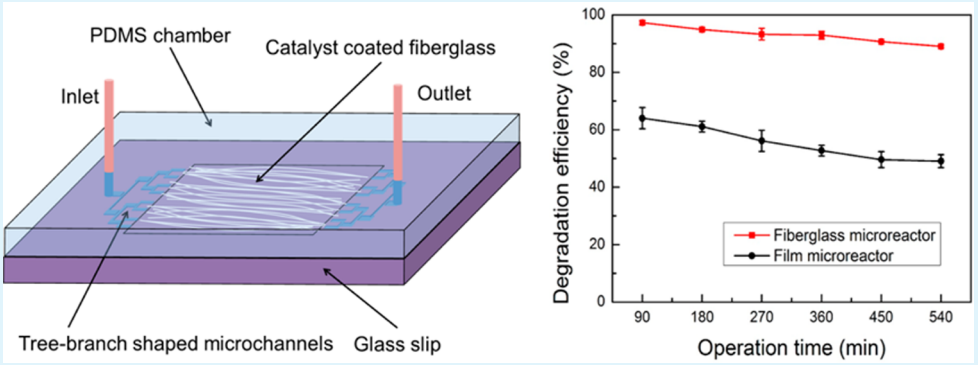

ABSTRACT: Optofluidic microreactors are promising prospects for photocatalytic reactions. However, because the flow type in conventional designs is typically laminar, the mass transport mainly relies on diffusion, and thus the rate of mass transport is limited. Accordingly, poor mass transport reduces the photocatalytic reaction rate. To alleviate the limitation of mass transport, in this work, we proposed a novel optofluidic microreactor with TiO_2-coated fiberglasses immersed in the microreaction chamber. Such a design enables enhanced mass transport by shortening the transport length and inducing the perturbation to liquid flow so as to improve the performance. We demonstrated the feasibility of the optofluidic microreactor with the TiO_2-coated fiberglass by the photocatalytic water treatment of methylene blue under UV irradiation. Results showed that the proposed optofluidic microreactor yielded much higher degradation efficiency than did the conventional optofluidic microreactor as a result of enhanced mass transport. The microreactor with the TiO_2-coated fiberglass showed a 2−3-fold improvement in the reaction rate constant as opposed to conventional ones. The maximal increment of the degradation efficiency can reach more than 40%.

KEYWORDS: *optofluidic microreactor, TiO_2-coated fiberglass, photocatalytic reaction, mass transport, degradation efficiency*

1. INTRODUCTION

Optofluidics is an emergent technology that combines microfluidics and modern optics in the same platform to leverage specific advantages of these two disciplines, such as fine flow control, large surface-area-to-volume ratio, and short light path.[1−3] These intrinsic features of optofluidics allow it to be used in a broad range of applications including chemical synthesis,[4] environmental protection,[5] energy production,[6] drug delivery,[7] online analysis,[8] and other aspects.[9] In recent years, because optofluidic microreactors can not only enable an intense and uniform light distribution by improving the photon transport but also realize an adequate interaction between fluid and light through enhancing the mass transport, the application of optofluidics to photoreaction and chemical reaction systems received wide attention. As mass and photon transport significantly affect the rate of photoreaction and chemical reaction, this new technology of an optofluidic microreactor is well suited for such systems to increase the reaction rates.[10]

Photocatalytic wastewater treatment of pollutants from textile industries is a typical photoreaction system. In a conventional reactor, such water treatment systems are typically implemented by large closed reactors with the catalyst suspended in the solution.[11] In this strategy, photocatalysts need to be recovered at the downstream by centrifuges, filters, and washing and then are reused, which greatly increases the capital and operational costs. To solve this problem, another strategy was proposed by direct coating of the catalyst onto the reactor inner surfaces or built-in structures.[12−15] In such reactors, however, not only is the photon transport poor but also the rate of mass transport is low as a result of large mass-transport resistance, both of which decrease the photocatalytic reaction rate. Luckily, it has been found that the above-limiting factors in the present reactors can be overcome by the optofluidic microreactor because of the above-mentioned advantages, which has been demonstrated by several reports.[16−18] For example, Erickson et al. designed an optofluidic microreactor to study the photocatalytic water splitting and demonstrated that such a platform had the

Received: September 6, 2013
Accepted: November 21, 2013
Published: November 21, 2013

potential to enhance the reaction rate.[19] Lei et al. proved that the reaction rate constant of the optofluidic microreactor was 100 times greater than that of the bulk reactor.[20] Moreover, optofluidic microreactors are able to realize the photocatalytic reaction within a few seconds rather than the typically several hours in large-scale reactors.[21−23]

Although promising, current designs of the optofluidic microreactor still face a major problem; i.e., the mass-transport capacity is unsatisfied because the flow type in optofluidic microreactors is typically laminar and mass transport mainly relies on diffusion, which hinders further improvement in the photocatalytic reaction rate. Under such circumstances, the development of a new optofluidic microreactor with a high mass transport rate is of importance in reality. In the present study, a novel optofluidic microreactor with TiO_2-coated fiberglass (termed the fiberglass microreactor) was proposed to enhance mass transport in the microreactor. The feasibility of this design was demonstrated by the photocatalytic degradation of methylene blue under UV irradiance.

2. NEW DESIGN OF THE OPTOFLUIDIC MICROREACTOR

As discussed above, the enhancement of mass transport is essential to improve the performance of current optofluidic microreactors. To this end, a new design of the optofluidic microreactor was proposed in this work, as sketched in Figure 1. Unlike the conventional layout in which the catalysts were coated on the microchamber inner surface, in this new design, the catalysts were coated onto the surface of the fiberglass and then the catalyst-coated fiberglasses were loaded into the optofluidic microreactor. As shown, this optofluidic microreactor was composed of a reaction microchamber containing catalyst-coated fiberglass and two micropores as the inlet and outlet. At both the inlet and outlet, tree-branch-shaped microchannels were adopted to ensure a uniform filling over the entire reaction microchamber. During the working process, reactants transport to the surface of the photocatalyst-coated fiberglass, on which the photocatalytic reactions occur.

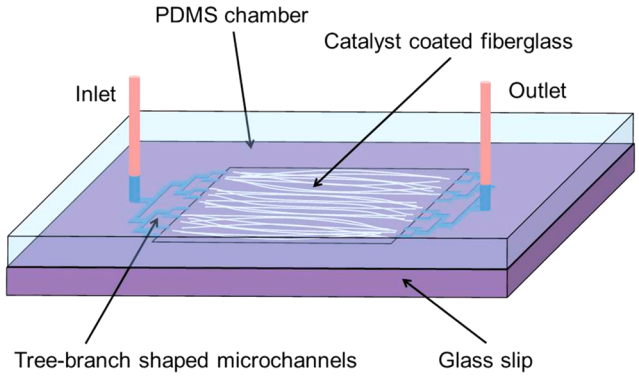

Figure 1. Schematic of the optofluidic microreactor with the catalyst-coated fiberglass.

Such a design provides two unique merits. The first one is the short transport length. The catalyst-coated fiberglass was suspended in the microreactor. Reactants only need to transport to the catalyst surface of the suspended fiberglass instead of the microchamber surfaces, shortening the transport length and thereby enhancing mass transport. The second one is the induction of perturbation to the liquid flow. The catalyst-coated fiberglass was suspended in the microreaction chamber with a random structure. Perturbation to the liquid flow can be created, further enhancing mass transport. Consequently, the mass transport capacity in this new optofluidic microreactor can be dramatically improved, thereby accelerating the photocatalytic reaction rate.

3. EXPERIMENTAL SECTION

3.1. Fabrication of TiO_2-Coated Fiberglass. The nanocatalyst of TiO_2 (Degussa P25, the mean size of primary particles is 25 nm) was used for the degradation of methylene blue (MB) in this work. The TiO_2-coated fiberglass was prepared by a sol−gel method,[24] which included two stages: preparing the TiO_2 colloid and coating TiO_2 on the fiberglass. In the first stage, 12 g of TiO_2 nanoparticles was dispersed in the mixture of 120 mL of deionized (DI) water and 0.4 mL of acetylacetone (Sigma-Aldrich) with magnetic stirring. Then 0.2 mL of Triton X-100 was added to facilitate the spreading of the colloid. After that, 2.4 g of poly(ethylene glycol) was added to the solution. The solution was then mixed for 12 h. In the second stage, a bundle of fiberglass was stretched in a glass dish. Ethanol was added to disperse the fiberglass, and then the fiberglass was dried under 80 °C for 5 min. Next, the prepared TiO_2 colloid was diluted by ethanol and then added into the glass dish. The fiberglass was soaked in the colloid for 50 min to allow the nanocatalysts to be adsorbed onto the surface of the fiberglass. At last, the fiberglasses were collected and dried in air at 80 °C for 1 h, which was followed by calcination in air for 2 h at 500 °C to form the catalyst-coated fiberglass.

3.2. Optofluidic Microreactor Fabrication. Poly(dimethylsiloxane) (PDMS) is a typical material to fabricate optofluidic microreactors because of its wide merits such as optical transparence, chemical inertness, and easy and rapid fabrication. In this experiment, the optofluidic microreactor was made by PDMS and a glass slide. The fiberglass coated with TiO_2 was sealed between the PDMS chip and a glass cover. The PDMS layer with a built-in microchamber was fabricated by the replica molding method in two steps.[25] In the first step, a master mold was prepared from the designed patterns by following the photolithography process. A negative photoresist (SU-8, MicroChem) was first spun onto a silicon wafer and prebaked. Next, the wafer with the photoresist was exposed to UV light through a printed mask with the designed patterns. After the soft-bake, the unexposed photoresist was removed with a developer solvent to form the master mold, which was then postbaked for 20 min. The resulting SU-8 height was 250 μm, corresponding to the depth of the microchamber. In the second step, the PDMS chip was formed on the developed master mold. A polymer base (Sylgard 184 A, Dow Corning) and curing agent (Sylgard 184 B, Dow Corning) were mixed at a ratio of 10:1 and degassed. Then, the mixture was cast onto the patterned wafer and baked at 95 °C for 120 min. After that, PDMS was released from the patterned wafer and cut into a chip. Finally, the developed PDMS chip was plasma-treated in air and bound to a glass slide loaded with the prepared catalyst-coated fiberglass to form an optofluidic microreactor with a 50 μL reaction microchamber (2.0 cm length, 1.0 cm width, and 250 μm height) and tree-branch-shaped microchannels connected to the inlet and outlet micropores. A detailed fabrication procedure and the image of the fabricated optofluidic microreactor are given in parts a and b of Figure 2, respectively.

In this study, to evaluate the performance of the developed optofluidic microreactor with catalyst-coated fiberglass, a conventional planar microreactor was also fabricated as a reference. In this reference microreactor, TiO_2 nanocatalysts were directly coated onto the inside surface of the glass slide cover instead of the fiberglass to form a planar film (termed the film microreactor). The fabrication procedure included the preparation of a TiO_2 colloid, dilution of the prepared colloid by ethanol, spraying of the diluted colloid onto the glass slide followed by drying at 80 °C, and finally calcining in air for 2 h at 500 °C. The active surface area on the glass slide was 2.0 cm^2 (1.0 cm × 2.0 cm), and the total catalyst loading was about 130 μg. Correspondingly, 220 catalyst-coated fiberglasses with a length of 2.0 cm were added

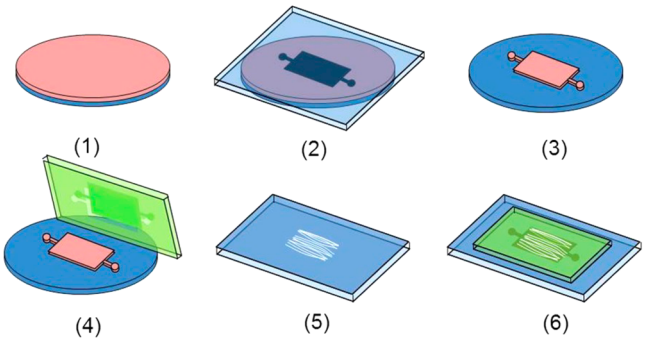

(a)

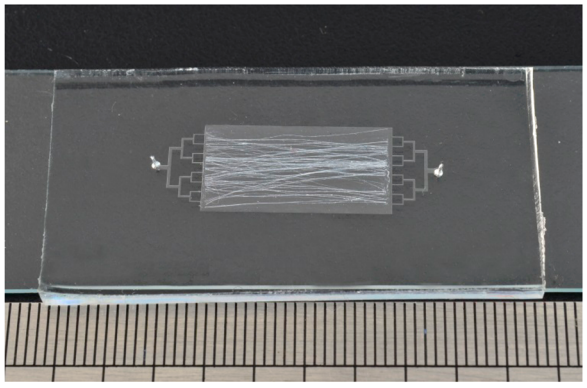

(b)

Figure 2. (a) Fabrication procedure of a PDMS/glass-based optofluidic microreactor with the catalyst-coated fiberglass. (b) Image of a fabricated optofluidic microreactor with the catalyst-coated fiberglass.

into the fiberglass microreactor, which resulted in the same total catalyst loading and active surface area as the film microreactor.

3.3. Experiment Setup. To demonstrate the feasibility of the developed optofluidic microreactor, MB, which is a common residual in wastewater from the textile industry, was used as a contaminant for water treatment. In this study, MB was dissolved into DI water and the pH value was maintained at 7.0. During the experiment, two syringe needles were connected to the inlet and outlet micropores. The prepared MB solution was introduced into the optofluidic microreactor by a syringe pump (LSP04-1A, Longer) through the needle. The optofluidic microreactor was illuminated by a 150 W mercury lamp with a wavelength range of 310−400 nm to ensure photocatalytic reactions. In addition, to avoid the temperature effect caused by illumination, the optofluidic microreactor was kept in a cooling bath to control the operating temperature. The UV illumination intensity was measured by a UV radiometer (UV-A, Photoelectric Instrument Factory of Beijing Normal University, China). The MB concentrations were characterized by the absorption spectra using a UV−visible spectrophotometer (TU-1901, Persee) at a wavelength of 664 nm, which corresponds to the absorbance peak of MB. Both microreactors were operated for 1 h to reach the absorption balance before normal experiments. Each experiment was repeated four times. Student's *t*-tests ($P < 0.05$) were performed for all experimental results, and error bars represent standard deviations from the average value.

4. RESULTS AND DISCUSSION

4.1. Morphology of TiO_2-Coated Fiberglass. The catalyst loading of a TiO_2-coated fiberglass was 0.68 $\mu g \cdot mm^{-2}$ with respect to the fiberglass outer surface, its morphology was characterized using scanning electron microscopy (SEM), and the results are shown in Figure 3 (left). It can be seen that TiO_2 nanoparticles were uniformly coated on the surface of the

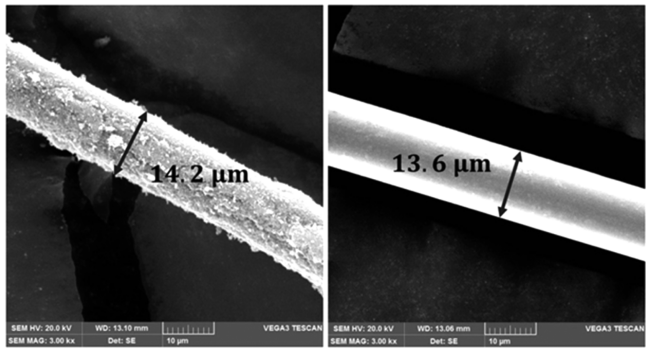

Figure 3. SEM images of the fiberglass with TiO_2 catalyst (left) and without TiO_2 catalyst (right).

fiberglass. Figure 3 (right) shows the SEM image of the fiberglass without TiO_2. The diameters of the fiberglass with and without TiO_2 were 14.2 and 13.6 μm, respectively, concluding that the thickness of the catalyst layer was about 0.3 μm.

4.2. Comparability of the Durability. The durability is a key parameter to represent the performance of the microreactor. Hence, both fiberglass and film microreactors were operated over a long period to assess this feature. In the testing, a MB solution with a concentration of 2×10^{-5} M was introduced into microreactors at a flow rate of 33.3 $\mu L \cdot min^{-1}$ and irradiated under a UV irradiance of 2 $mW \cdot cm^{-2}$. For the film microreactor, light was irradiated from the top to the TiO_2 film through the fluidic layer. The degradation efficiencies of both microreactors were measured after operations of 90, 180, 270, 360, 450, and 540 min, respectively. Because these two microreactors had the same catalyst loading, active surface area, and microchamber dimensions, the difference between these two microreactors mainly relies on the mass transport capacity, resulting from their respective intrinsic structures.

Variation of the degradation efficiency with the operation time is compared in Figure 4. As shown, the degradation efficiency of both microreactors declined slowly as the operation time increased. For the fiberglass microreactor, the

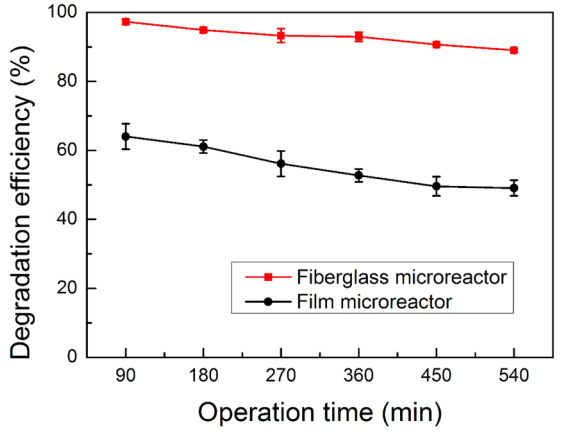

Figure 4. Degradation of MB as a function of the operation time. MB concentration: 2×10^{-5} M. Flow rate: 33.3 $\mu L \cdot min^{-1}$. Residence time: 90 s. Fiberglass quantity: 220.

degradation efficiency decreased from 97.3 ± 0.7% to 89.0 ± 0.5%, while a reduction from 64.0 ± 3.7% to 48.1 ± 2.3% for the film microreactor was observed. The decrease in the degradation efficiency of these two microreactors can be attributed to the intermediates produced by photocatalytic reactions. During the MB degradation process, the intermediates produced by photocatalytic reactions adsorbed on the catalytic surfaces, lowering the active surface area. The lowered active surface area slowed the photocatalytic reaction rate and thus decreased the efficiency. As time progressed, coverage by the intermediates slowly upgraded so that the degradation efficiency gradually decreased. Once production and removal of the intermediates reached a balance, the degradation efficiency became relatively stable. More importantly, it can be seen from Figure 4 that the degradation efficiency of the fiberglass microreactor could reach 90%, which was much higher than that of the film microreactor. Because the catalyst loading and active surface area were the same in these two microreactors, enhancement of the degradation efficiency for the fiberglass microreactor can be solely attributed to the reasons mentioned in the preceding section. The addition of the catalyst-coated fiberglass into the microreactor not only shortens the diffusion length but also induces perturbation to the liquid flow, enhancing mass transport. Enhanced mass transport increased the MB concentration at the active surface, which facilitates the photocatalytic reaction and thereby improves the degradation efficiency. Besides, enhanced mass transport also benefits product removal. As a result, more active sites can be exposed to MB for the photocatalytic reactions, further improving the microreactor performance. In addition, it was found that the fiberglass microreactor still showed a high degradation efficiency after 9 h of operation, indicating that the new optofluidic microreactor has good durability. The above facts fully demonstrate the feasibility of the developed optofluidic microreactor with the catalyst-coated fiberglass.

4.3. Effect of the Flow Rate. Variation in the flow rate can cause changes in the microreactor performance. For this reason, the effect of the flow rate was investigated. In this experiment, the feeding MB concentration was 2×10^{-5} M and the UV irradiance intensity was kept at 2 mW·cm^{-2} . The flow rate ranged from 33.3 to 200 μL·min^{-1}, which can be represented by the residence time. According to the relationship between the flow rate and residence time of the MB solution

$$\text{residence time} = \text{chamber volume}/\text{flow rate} \quad (1)$$

where the chamber volume was 50 μL as given, corresponding residence times of 90, 60, 45, 30, and 15 s were determined, respectively. A large residence time corresponds to a low flow rate.

Figure 5a shows variation in the degradation efficiencies of both microreactors. Clearly, upgrading the residence time led to an increase in the degradation efficiency of both optofluidic microreactors. It is easy to understand that larger residence time means longer staying time in the microreactor, which makes MB more effectively contact the catalyst. On the other hand, larger residence time lowered the load to the system, which also contributes to high degradation efficiency. More interestingly, the degradation efficiency of the fiberglass microreactor remained at a high level, which was almost twice as much as that of the film microreactor. It just took 15 s for the fiberglass microreactor to degrade 45% MB but 75 s for the film microreactor. No doubt, this is due to the internal structure of the immersed catalyst-coated fiberglass that greatly

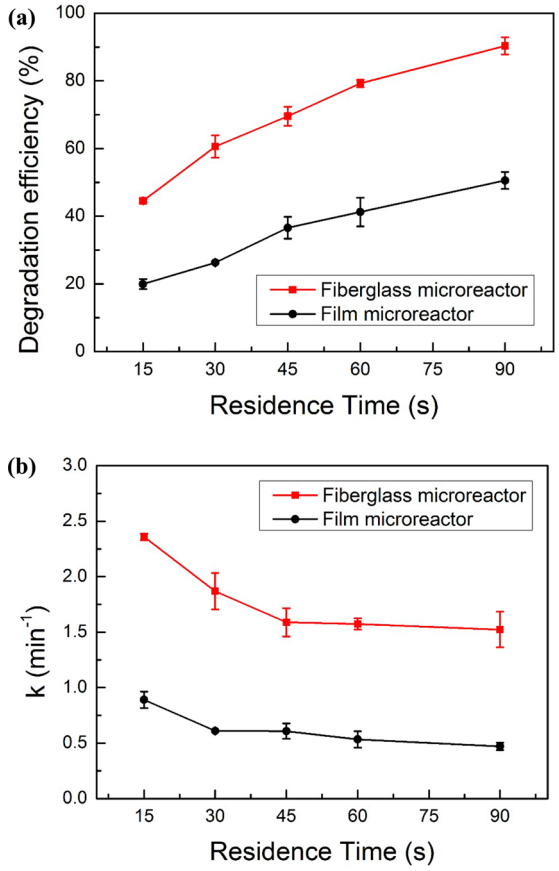

Figure 5. (a) Effect of the residence time on the degradation efficiency. (b) Variation of the reaction rate constant with the residence time. MB concentration: 2×10^{-5} M. Fiberglass quantity: 220.

reduced the mass transport resistance of reactant transport and product removal in the fiberglass microreactor. In particular, operating the optofluidic microreactors at large residence time caused the mass transport capability to be intrinsically weak because of the low flow rate. Under such circumstances, therefore, the enhancement of mass transport by using the catalyst-coated fiberglass in the new design of the optofluidic microreactor became more obvious. Subsequently, the difference in the degradation efficiency between these two microreactors increased with the residence time, and the improvement in the degradation efficiency became most significant at a residence time of 90 s.

The reaction rate constant is an important parameter describing the photocatalytic reaction rate. In general, the reaction rate constant mainly depends on two factors: the intrinsic reaction rate and the mass transport rate of MB from the liquid to the catalyst surface.[26] In the experiment, because the reactants, catalyst type and loading, active surface area, and other conditions were the same, variation of k is mainly associated with the mass transport capacity. For this reason, to gain deep insight into the enhancement of mass transport by the fiberglass microreactor, the reaction rate constant k was also discussed, which can be determined from the degradation efficiency of each microreactor as follows:[26]

$$k = -\ln(1 - x)/t \quad (2)$$

where x is the degradation efficiency and t stands for the residence time. Figure 5b shows the reaction rate constants of

the fiberglass and film microreactors against the residence time. It is shown that k of the fiberglass microreactor was much higher than that of the film microreactor. This is mainly attributed to the enhanced rates of reactant transfer and product removal. In addition, it was also found that the reaction rate constants of both microreactors decreased with an increase of the residence time. It decreased from 2.36 ± 0.05 and 0.89 ± 0.12 to 1.52 ± 0.26 and 0.47 ± 0.05 min^{-1} for the fiberglass and film microreactors, respectively. This is because the small residence time corresponding to the high flow rate helps to improve mass transport, which accelerates the reaction rate. In summary, analysis of the reaction rate constant further demonstrates that the new design of the optofluidic microreactor can dramatically enhance mass transport.

4.4. Effect of the MB Concentration. The effect of the MB concentration is shown in Figure 6a. In this testing, the MB concentration ranged from 0.3×10^{-5} to 3×10^{-5} M. The flow rate of the MB solution was kept at 66.6 $\mu L \cdot min^{-1}$, and the intensity of UV irradiance was 2 $mW \cdot cm^{-2}$. In addition, a microreactor with the same reactor dimensions but without TiO_2 was also fabricated to visit the effect of UV irradiation itself on the degradation of MB. It can be found from Figure 6a that, as the MB concentration increased, the degradation efficiency of the fiberglass microreactor declined from 90.5 ± 4.1% to 72.0 ± 2.6% and the degradation efficiency of the film microreactor dropped from 64.3 ± 1.7% to 29.1 ± 4.4%.

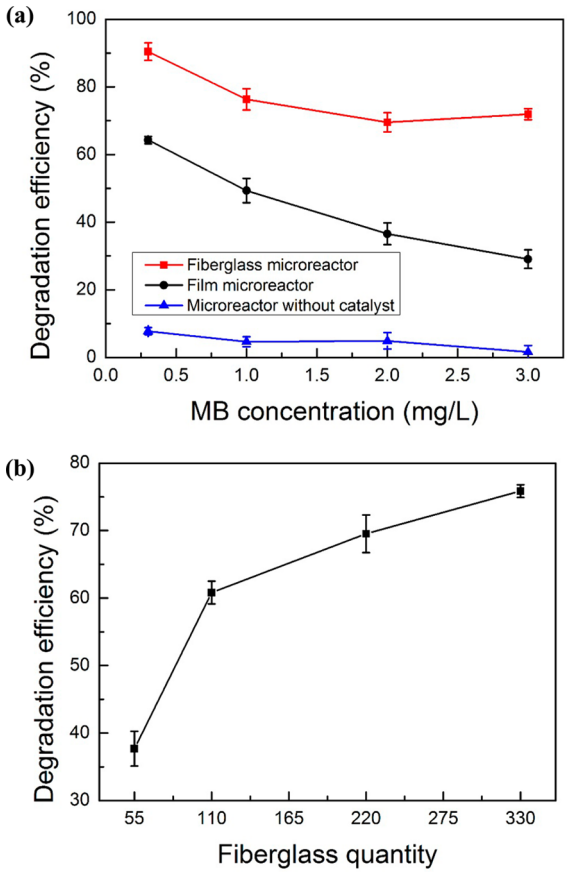

Figure 6. (a) Effect of the MB concentration on the degradation efficiency. Flow rate: 66.6 $\mu L \cdot min^{-1}$. Residence time: 45 s. Fiberglass quantity: 220. (b) Effect of the fiberglass quantity on the degradation efficiency. MB concentration: 2×10^{-5} M. Flow rate: 66.6 $\mu L \cdot min^{-1}$. Residence time: 45 s.

However, for the microreactor without catalyst, the degradation efficiency was always low (<10%), implying that, in cases with catalysts, the contribution from the MB degradation only by UV irradiation can be ignored in this study. For the fiberglass and film microreactors, reduction of the degradation efficiency can be attributed to three aspects. First, increasing the MB concentration increases the load to the optofluidic microreactor. On the other hand, the capabilities of the microreactors are limited so that high MB concentration yielded low degradation efficiency. Second, despite the fact that the higher MB concentration is beneficial for the photocatalytic reaction, more intermediates are simultaneously generated, which adsorb on the active surfaces of the catalysts. As such, a significant amount of active surface area was covered at high-MB-concentration operation, hindering the reaction between photogenerated holes or hydroxyl radicals and reactants and thereby lowering the degradation efficiency. Third, with an increase of the MB concentration, photon transfer is limited by the optical attenuation in the MB solution, which also lowers the photocatalytic reaction rate and thus the degradation efficiency. Because of these three reasons, the degradation efficiency decreased with increasing MB concentration.

Although both the fiberglass and film microreactors exhibited the same descending trend with an increase in the MB concentration, the performance of the fiberglass microreactor was much better than that of the film microreactor as a result of enhanced mass transport. Besides, higher MB concentration exhibited larger improvement of the degradation efficiency because high-MB-concentration operation resulted in more intermediates to be produced. Poison to photocatalysts becomes severe. On the other hand, the optical attenuation in the reactants at high MB concentration exerts more critical influence. In this case, enhanced mass transport can not only decrease the coverage by intermediates to accelerate the photocatalytic reactions but also weaken the optical attenuation. Hence, the improvement in the degradation efficiency becomes more significant. This fact indicates that, in addition to the superior performance, the fiberglass microreactor has more operation range in real applications.

4.5. Effect of the Fiberglass Quantity. The quantity of the catalyst-coated fiberglass is another important factor because it determines the catalyst loading, active surface area, and resulting internal structure in the microchamber that ultimately determines the performance of the fiberglass microreactor. To study the effect of the fiberglass quantity, several fiberglass microreactors with various fiberglass quantities ranging from 55 to 330 were fabricated and tested. The resulting total catalyst loadings were about 33, 66, 130, and 200 μg, respectively, which corresponded to active surface areas of about 0.5, 1.0, 2.0, and 3.0 cm^2, respectively. The other conditions were a MB solution of 2×10^{-5} M, a flow rate of 66.6 $\mu L \cdot min^{-1}$, and a UV irradiance density of 2 $mW \cdot cm^{-2}$. The experimental results are presented in Figure 6b, which shows that the degradation efficiency improved with an increase of the catalyst-coated fiberglass quantity. This is because increasing the catalyst-coated fiberglass quantity increased the total catalyst loading and the corresponding reaction area. As a result, the degradation efficiency was improved. On the other hand, an increase of the fiberglass quantity makes the inner structure more complex and can induce stronger perturbation to the liquid flow, which also facilitates mass transport and thus the photocatalytic reactions. In addition, it was also found that the degradation efficiency sharply ascended from 37.7 ± 4.1%

to 60.8 ± 2.7% when the fiberglass quantity increased from 55 to 110. It is indicated that doubling the fiberglass quantity in this range can dramatically increase the active surface area and enhance mass transport. Therefore, the degradation efficiency was greatly improved. From Figure 6b, it can also be seen that, as the quantity of the catalyst-coated fiberglass was further increased from 110 to 330, the degradation efficiency increased just from 60.8 ± 2.7% to 76 ± 1.2%, indicating that enhancement by enlarging the active surface area becomes weak and the enhanced mass transport of MB may approach the limitation. Consequently, the optofluidic microreactor with high fiberglass quantity showed small improvement in the performance. However, it should be recognized that, for the film microreactor, increasing the catalyst loading may not show significant improvement in the performance because the active surface area may not be greatly enlarged because of the planar design. Therefore, the optofluidic microreactor with catalyst-coated fiberglass provides a feasible approach that not only enlarges the reaction area but also enhances mass transport.

5. CONCLUSION

In this study, a novel optofluidic microreactor with photocatalyst coated on the fiberglass was developed. The feasibility of this new design was demonstrated by the photocatalytic water treatment toward MB under UV irradiation. Experimental results revealed that, compared with the conventional planar film-designed optofluidic microreactor, the optofluidic microreactor with the catalyst-coated fiberglass can dramatically improve the microreactor performance as a result of enhanced mass transport by shortening the diffusion transport length and inducing perturbation to the liquid flow. The effects of different parameters including the flow rate, MB concentration, and fiberglass quantity were also visited to evaluate the performance of the proposed optofluidic microreactor. Our results showed that low flow rate and MB concentration and large fiberglass quantity could yield high degradation efficiency. Besides, with the proposed optofluidic microreactor, the reaction rate constant could be increased 2−3 times because of the high mass-transport rate. In addition to the enhancement of mass transport, this design of the catalyst-coated fiberglass could significantly enlarge the reaction area in the optofluidic microreactor for given catalyst loading. These unique features also allow this new design to be potentially applied to other photoreaction systems such as water splitting, photoreduction of CO_2, air purification, and so on.

AUTHOR INFORMATION

Corresponding Author

*Tel.: 0086-23-65102474. Fax: 0086-23-65102474. E-mail: rchen@cqu.edu.cn.

Notes

The authors declare no competing financial interest.

ACKNOWLEDGMENTS

The authors gratefully acknowledge financial support from Chongqing Natural Science Foundation for Outstanding Young Scholars (Grant CSTC2012JJJQ90003), Natural Science Funds for Distinguished Young Scholar of Chongqing (Grant 51222603), National Natural Science Foundation of China (Grants 51106188 and 51276208), Natural Science Foundation of Chongqing, China (Grant CSTC2011BB4071), and the Fundamental Research Funds for the Central Universities (Grants CDJZR12148801 and CDJZR12140028).

REFERENCES

(1) Erickson, D.; Sinton, D.; Psaltis, D. *Nat. Photonics* **2011**, *5*, 583−590.
(2) Fan, X.; White, I. M. *Nat. Photonics* **2011**, *5*, 591−597.
(3) Cuennet, J.; Vasdekis, A.; De Sio, L.; Psaltis, D. *Nat. Photonics* **2011**, *5*, 234−238.
(4) Haswell, S. J.; Watts, P. *Green Chem.* **2003**, *5*, 240−249.
(5) Gardeniers, J.; Van den Berg, A. *Anal. Bioanal. Chem.* **2004**, *378*, 1700−1703.
(6) Eunjungá Jung, E.; Devin, F. *Lab Chip* **2012**, *12*, 3740−3745.
(7) Dittrich, P. S.; Manz, A. *Nat. Rev. Drug Discovery* **2006**, *5*, 210−218.
(8) Gao, Y. a.; Li, N.; Zheng, L.; Zhao, X.; Zhang, S.; Han, B.; Hou, W.; Li, G. *Green Chem.* **2006**, *8*, 43−49.
(9) Medina-Sánchez, M.; Miserere, S.; Merkoçi, A. *Lab Chip* **2012**, *12*, 1932−1943.
(10) Shannon, M. A.; Bohn, P. W.; Elimelech, M.; Georgiadis, J. G.; Mariñas, B. J.; Mayes, A. M. *Nature* **2008**, *452*, 301−310.
(11) Tayade, R. J.; Natarajan, T. S.; Bajaj, H. C. *Ind. Eng. Chem. Res.* **2009**, *48*, 10262−10267.
(12) Mahmoodi, N. M.; Arami, M.; Limaee, N. Y. *J. Hazard. Mater.* **2006**, *133*, 113−118.
(13) Sun, R.-D.; Nakajima, A.; Watanabe, I.; Watanabe, T.; Hashimoto, K. *J. Photochem. Photobiol., A* **2000**, *136*, 111−116.
(14) Danion, A.; Disdier, J.; Guillard, C.; Jaffrezic-Renault, N. *J. Photochem. Photobiol., A* **2007**, *190*, 135−140.
(15) Wang, W.-Y.; Irawan, A.; Ku, Y. *Water Res.* **2008**, *42*, 4725−4732.
(16) Gorges, R.; Meyer, S.; Kreisel, G. *J. Photochem. Photobiol., A* **2004**, *167*, 95−99.
(17) Lu, H.; Schmidt, M. A.; Jensen, K. F. *Lab Chip* **2001**, *1*, 22−28.
(18) Wang, N.; Zhang, X.; Chen, B.; Song, W.; Chan, N. Y.; Chan, H. L. *Lab Chip* **2012**, *12*, 3983−3990.
(19) Ahsan, S. S.; Gumus, A.; Erickson, D. *Lab Chip* **2013**, *13*, 409−414.
(20) Lei, L.; Wang, N.; Zhang, X.; Tai, Q.; Tsai, D. P.; Chan, H. L. *Biomicrofluidics* **2010**, *4*, 043004.
(21) Malato, S.; Blanco, J.; Vidal, A.; Alarcón, D.; Maldonado, M. I.; Cáceres, J.; Gernjak, W. *Sol. Energy* **2003**, *75*, 329−336.
(22) Ray, S.; Lalman, J. A.; Biswas, N. *Chem. Eng. J.* **2009**, *150*, 15−24.
(23) Benotti, M. J.; Stanford, B. D.; Wert, E. C.; Snyder, S. A. *Water Res.* **2009**, *43*, 1513−1522.
(24) Nazeeruddin, M.; Kay, A.; Rodicio, R.; Miiller, E.; Liska, P. *J. Am. Chem. Soc* **1993**, *115*, 6382−6390.
(25) Hong, J. W.; Fujii, T.; Seki, M.; Yamamoto, T.; Endo, I. *Electrophoresis* **2001**, *22*, 328−333.
(26) Lin, H.; Valsaraj, K. T. *J. Appl. Electrochem.* **2005**, *35*, 699−708.